Ocean Science Journal, Vol. 42 No. 3, 153-163(2007)

Article

Ocean Science Journal

http://osj.kordi.re.kr

Numerical Modeling of Tide and Tidal Current in the Kangjin Bay, South Sea, Korea

Young Jae Ro[1]*, Woong Sik Jun[2], Kwang Young Jung[1], and Hyun Min Eom[3]

[1]*Department of Oceanography, College of Natural Sciences, Chungnam National University, Taejon 305-764, Korea*

[2]*Dawoo Ocean Corporation, Daebang-dong 389-23 Dongjak-gu , Seoul 156-810, Korea*

[3]*Technology R&D Institute, Hyein E&C Co. Ltd., Singil 7-dong 761, Yeongdeungpo-gu, Seoul 150-854, Korea*

Received 14 June 2007; Revised 10 August 2007; Accepted 13 September 2007

Abstract – This study is based on a series of numerical modeling experiments to understand the tidal circulation in the Kangjin Bay (KB). The tidal circulation in the KB is mostly controlled by the inflow from two channels, Noryang and Daebang which introduce the open ocean water into the northern part of the KB with relatively strong tidal current, while in the southern part of the KB, shallowest region of the entire study area, weak tidal current prevails. The model prediction of the sea level agrees with observed records at skill scores exceeding 90 % in terms of the four major tidal constituents (M2, S2, K1, O1). However, the skill scores for the tidal current show relatively lower values of 87, 99, 59, 23 for the semi-major axes of the constituents, respectively. The tidal ellipse parameters in the KB are such that the semi-major axes of the ellipse for M2 range from 1.7 to 38.5 cm/s and those for S2 range from 0.5 to 14.4 cm/s. The orientations of the major-axes show parallel with the local isobath. The eccentricity values at various grid points of ellipses for M2 and S2 are very low with 0.2 and 0.06 on the average, respectively illustrating that the tidal current in the KB is strongly recti-linear. The magnitude of the tidal residual current speed in the KB is on the order of a few cm/s and its distribution pattern is very complex. One of the most prominent features is found to be the counter-clockwise eddy recirculation cell at the mouth of the Daebang Channel.

Key words – numerical model, tide, ellipse parameter, Kangjin Bay, South Sea

1. Introduction

The Study area is located in the central part of the South Sea of Korea, called the Kangjin Bay (hereafter, KB) which is a typical semi-enclosed embayment characterized by its complexity of physical settings, ie, complicated coastline, fresh water inputs from the Sumjin River and the Namgang Dam (NG Dam) from the north, two channels of the Changson (CS) Channel and the Daebang (DB) Channel connecting to the South Sea (Fig. 1a). The bottom topography in the KB is very shallow, with average depth of 8.9 m with deeper area in the northwest which is connected to the Noryang (NR) Channel. The averaged annual discharge of the Sumjin River is about 120 m^3/sec. Yet, in the summer monsoon season, the fresh water discharge from the NG Dam reached up to 3523 m^3/sec on August 19, 2004.

Little attention had been paid to the study area (KB) until the research project launched in Sept. 2003 by Ro (2006), and thus the area has been poorly investigated, especially considering its important geographical location, the significant roles of its physical processes, and its impact on the ecosystem of the KB. The significance of the study of the KB lies in two aspects; firstly, to understand the tidal and density-driven circulation in the complex system consisting of the geometry, river runoffs, and tide, and secondly, to understand the ecosystem problems, since this area is renowned for aqua-culturing beds for several important shellfish species such as large-arc shell (*Scapharca broughtonii*) and short-necked clam (*Tapes philippinarum*) *et al.*

The database for the water quality, current and meteorological conditions were collected *in situ* by establishing a realtime

*Corresponding author. E-mail: royoungj@cnu.ac.kr

monitoring system, which continuously monitored with very high sampling resolution 10 min. for the period of Apr., 2004 to August, 2006. Detailed technical information for the system can be referred to Ro and Choi (2004).

Characteristics of the tidal and residual current in the KB have been analyzed by the present author (Ro 2007). Numerous studies can be found on numerical modeling of tidal circulation in the coastal and estuarine environments throughout the world. Among these, some are particularly relevant to this study: Gomez-Valdes *et al.* (2003) investigated the generation of overtides and compound tides as the results of the dominant nonlinear processes in coastal water; Marinone and Lavin (2005) described the tidal ellipse parameters in the Gulf of California by using a 3D numerical model; McLaughlin *et al.* (2003) found the spring–neap residual modulation in the Great Bay. Numerical modeling experiments were conducted to investigate the influence of river runoff on the tidal circulation (McLaughlin *et al.* 2003; Horrevoetsa *et al.* 2004; Park *et al.* 2005; Ji *et al.* 2007; Levasseur *et al.* 2007) in various parts of estuarine waters in the world. Mechanism for the generation of the residual current was investigated by Marinone and Lavin (2005) and Cai *et al.* (2003).

In this study, we will provide and describe the results of a series of numerical modeling experiments designed to understand the tidal dynamics and density-driven current caused by the NG Dam water discharge, and its impact on the local fishery and eco-system. Since the scope of modeling experments are wide, we decided to provide the results in several separate parts: in Part I, characteristics of tide and tidal current in the KB are described, and, in Part II, density-driven circulation and formation of the stratification followed by the NG Dam water discharge in summer season is simulated; in Part III, wind-driven circulation and impact of the typhoon passage over the KB is simulated; and finally, in Part IV, the water quality and the formation of hypoxia is computed and simulated. The main objective of the Part I is to characterize the tidal current field in the KB in terms of tidal ellipse parameters, tidal residual current and the overall circulation pattern in the KB.

2. Numerical Model for the Kangjin Bay

Physical Settings and Bottom Topography

The KB, located in the center of the South Sea, is typical of Korean coastal embayment system which is characterized by its rugged and complicated coastline, often semi-enclosed by a headland which is interconnected with one or two river mouths and shallow in depth, mostly less than 20 (m), and with tidal flats developed in the near-shore area. As seen in Fig. 1a, the northern area of KB is composed of the NR Channel and Sachon Bay (SB) through which fresh water input is introduced from the NG Dam. In the middle part of KB lies the Jinju Bay (JB) which is connected to KB toward the southwest and to the DB Channel toward the southeast. For the convenience of description of the current field in section 3, the model domain is arbitrarily sub-divided into five sub-regions, namely NR, SC, KB, DB, and OW (ocean water).

The KB is the shallowest area in the entire domain, whereas the DB Channel and the CS Channel are very narrow so that the tidal current is intensified due to the bottle-neck effect both on ebb and flood phases. The two channels are important since they are connected to the open sea waters facing to the South Sea. The bottom in the KB is shallow with the exception of deeper parts in the South Sea area and subsurface valley in the northwestern part from the NR Channel. Average depth of the model grid points is 8.9 m with 70 % of grid points less than 10 m and the deepest grid point being 26.9 m.

The dynamics of the water circulation in the KB is, in general, dominated by the semi-diurnal tide, which is complicated by the coastal storm activity and fresh water runoff in the summer season whose impact on the circulation and vertical structure of the water column sometimes may well override the tidal current field in terms of the magnitude of velocity and the vertical structure of water column. The impact of the fresh water discharge into the KB will be of major subject in the next paper (Ro and Jung 2007).

Model Specification and Numerical Schemes

The model specifications of this study are as follows: the model domain for the KB is shown in Fig. 1b which encompasses three open boundaries and two sources of river runoff with very complicated coastline and three narrow channels, namely NR, CS and DB. The grid system for the model domain is composed of 95×126 grid cells with variable grid sizes from 100 to 400 m, with finer resolution in the channel area and three open boundaries. The 5 sigma levels evenly divided in the vertical

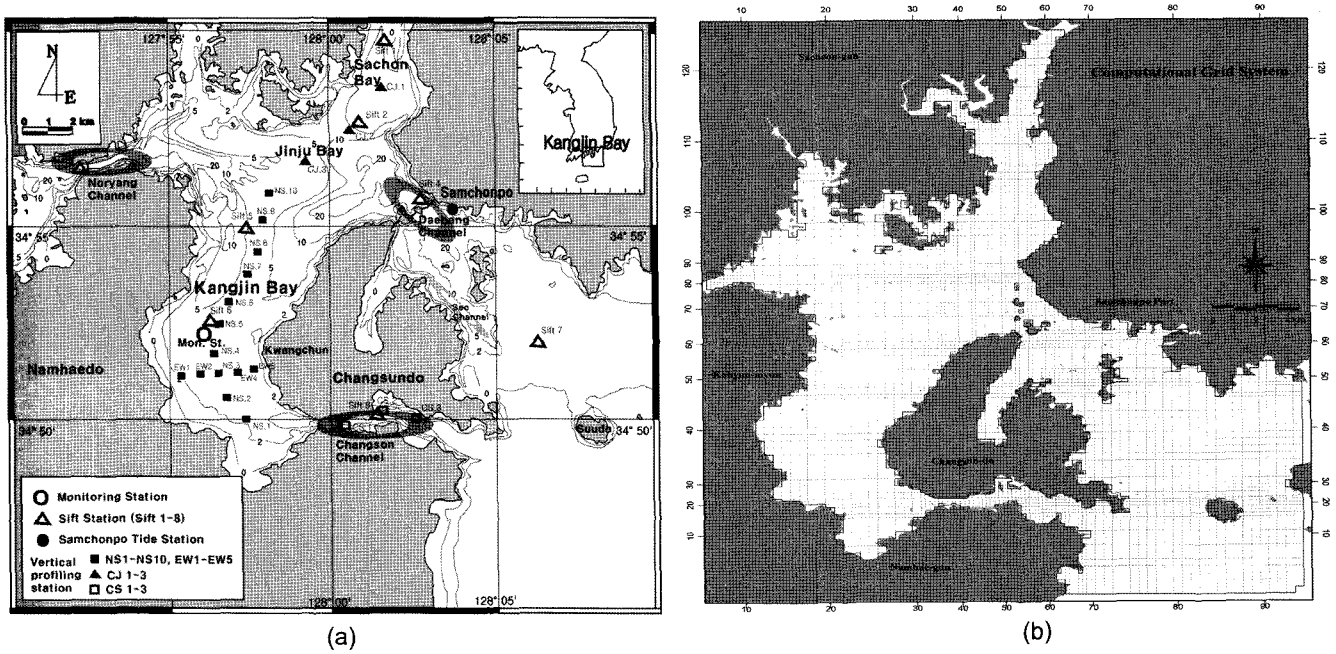

Fig. 1. (a) Map for the study area with locations for various stations and selected points, (b) Grid system for the numerical model for the Kangjin Bay, South Sea, Korea.

Table 1. Amplitude (m) and phases (deg.) of tidal constituents used for model forcings at open boundary points.

Boundary		Index	M2		S2		K1		O1	
			Amp.	Phase	Amp.	Phase	Amp.	Phase	Amp.	Phase
West	start	73	0.69	300	0.25	298	0.18	166	0.16	138
	end	78	0.7	301	0.26	299	0.18	166	0.16	139
East	start	2	1.0	250	0.39	289	0.16	151	0.12	123
	end	48	1.02	252	0.40	291	0.16	152	0.12	124
South	start	63	1.02	252	0.40	291	0.16	152	0.12	124
	end	94	1.0	250	0.39	289	0.16	151	0.12	123

Phase is relative to local meridional, 135°E

are designed so as to resolve the surface and bottom boundary layers as well as the surface-trapped river plume with resolution better than 0.5 m near the surface in most of the grid points (Fig. 1b).

The numerical model for the KB used in this study is ECOM3D, a three-dimensional, sigma coordinate, hydrostatic, primitive equation model derived from the Princeton Ocean Model (Blumberg and Mellor 1987). Since this model has been widely used, interested readers may refer to Kourafalou (1996a, b) or Fong (1998) or the POM homepage for detailed technical descriptions. The model includes a mode splitting technique for computational efficiency. The external and internal time steps are 10 seconds and 5 minutes respectively, in compliance with the CFL criterion. The horizontal mixing coefficients of salt, temperature and momentum are parameterized using the Smagorinsky (1963) formula, while the vertical mixing coefficients are parameterized using the 2.5-level closure scheme of Mellor and Yamada (1982). No salt and heat flux conditions are applied to the surface boundary. At the bottom, the quadratic bottom stress with a bottom drag coefficient is applied with no salt and heat fluxes and zero vertical velocity. The coastal wall boundary is impenetrable, impermeable and no-slip.

The model is initially prescribed with a homogeneous temperature of 20 °C and a salinity of 33.5 psu. On the open boundaries, the southern and western boundary conditions are imposed with tidal elevations composed of the 4 major tidal constituents. The drying-flooding procedure was taken into account for treating the area of intertidal

flats in the KB. Internal velocities are radiated out through the three open boundaries based on the radiation boundary condition following Orlanski (1976).

To force the model, amplitudes and phase lags for 4 major tidal constituents are imposed at the open boundary points listed in the Table 2. To determine the optimal open boundary conditions, co-tidal charts were referred to Odamaki (1989) and Matsumoto *et al.* (2000). Amplitude of M2 is about 100 cm along the southern and eastern boundaries and 70 cm along the western boundary. Various sensitivity experiments (results not presented in this paper) had been carried out to produce the best fitted model outputs to the sea level and current observations.

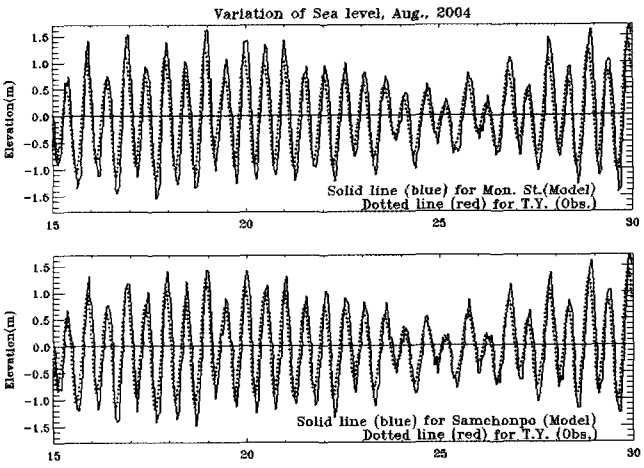

Fig. 2. Time series of elevations at Monitoring Station in the Kangjin Bay, at Samchonpo and at Tong-Young Station.

Field measurements and Datasets for Model Calibration and Validation

In carrying out the KB Project (Ro 2006), intensive field work had been carried out to produce the database by two methods: (1) the realtime monitoring system produced the hydrographic and hydrodynamic conditions such as water temperature and salinity, current speed and direction, meteorological parameter such as wind speed and direction, solar irradiance and humidity, etc every 10 minutes, and (2) bimonthly field observations made to obtain vertical profiles of hydrographic condition such as temperature, salinity and dissolved oxygen by using YSI (model 6600). In particular, current meter record (measured by the Aanderraa RCM 9) and water temperature, salinity and dissolved oxygen for the month of August, 2004 are used to compare with the model outputs.

The current meter records along with wind records over 500 days were obtained in the KB, South Sea, Korea, from March, 2003 to Nov. 2005 and analyses were carried out in detail by various analyses including descriptive statistics, harmonic analysis of tidal constituents, spectra and coherence, the principal axis, and progressive vector diagrams, (Ro 2007). In short, current speed in the KB ranges from -28 to 33 cm/sec, with standard deviations from 6.5 to 12.9 cm/sec. The harmonic analyses of the tidal currents show the average form number, 0.12 with semi-diurnal type and the recti-linear orientation of the major axis toward northeast. The magnitudes of the semi-major range from 12.7 to 17.7 cm/sec for M2 harmonics, while for S2 harmonics, they range from 6.3 to 10.4 cm/sec, respectively. Fig. 2 shows the time series of current records for the model experiments where, in general, the semi-diurnal tidal oscillation modulated by neap-spring tidal cycle is obvious and other non-tidal and sub-tidal components are inherent.

Harmonic analyses to estimate tidal constituents and tidal ellipse parameters were carried out based on the classical technique (Foreman 1978) by using the Matlab program package provided by Pawlowicz *et al.* (2002). Subsequently, tidal residual current of the model outputs was calculated by subtracting the tidal harmonics. In harmonic analyses, by choosing Rayleigh criterion of 1.0, 17 tidal constituents could be resolved with 16-day long model output. The frequencies of tidal constituents resolved by the harmonic analysis package range from 0.0028219 for MSF to 0.3220456 for M8 cph.

3. Simulation of Tidal Current

Model Assessment and Validation

Model test and run validation were carried out in the beginning phase of the modeling experimental efforts. Model performance tests and run validation are normally made through several steps; firstly, null model with zero forcing produced zero values for all variables. After we confirmed the first step, we proceeded to the next step where modelings with a chosen set of open boundary conditions were carried out. The model outputs would then be analyzed to assess the overall model performance in reproducing current field and sea level elevation. Field measurements of sea level and current were compared to model output. This step involved iterative modeling experiments

Table 2. (a) Comparison between model output of sea level and observations at two points in terms of 4 tidal constituents.

Constituent	Model				Observation				% Skill Samchonpo	
	Mon. St.		Samchonpo		Samchonpo		Tong-Young			
	amp	phase	amp	phase	amp	phase	amp	phase	amp	phase
M2	92.0	250.9	92.0	237.0	94.3	250.9	74.0	246.9	97.6	94.5
S2	46.7	272.6	43.1	275.8	46.7	272.6	36.7	277.2	92.3	98.8
K1	16.6	169.0	15.2	156.4	16.6	169.0	16.8	179.8	91.6	92.5
O1	12.2	152.7	12.4	122.3	12.2	152.7	10.4	142.9	98.4	80.1

(b) Non-harmonic constants for the model results and observation.

Non-harmonic constant		Model		Observation	
		Mon. St.	Samchonpo	Samchonpo	Tong-Young
Spring	High	306.2	297.8	310.8	248.5
	Low	28.8	27.6	28.8	27.2
	Range	277.4	270.2	282.0	221.3
Neap	High	212.8	211.5	217.4	175.1
	Low	122.2	113.9	122.2	100.5
	Range	90.6	97.6	95.2	74.6

until most convincing open boundary conditions were determined.

To assess the model skill quantitatively, we adopt the skill score suggested by Martin and McCutcheon (1999) which is defined as the deviation of the relative error from unity in the Eqn. (1).

$$\text{Skill} = 1\text{- relative error (RE)} \quad (1)$$

where $RE = abs(X_{model} - X_{obs}) / X_{obs}$

Here X can be any of amplitude, phase lag, or tidal ellipse parameters for the tidal elevation or velocity component. When we multiply skill score by 100, it can be called percentage skill (William and Thompson 2001). Percentage skill scores may range from 0 to 100, which correspond to no match and perfect match between model and observation.

The time series of sea level at the Mon. St., neighboring Samchonpo and Tong-Young (hereafter, TY) tidal stations are shown in Fig. 2. By comparing the model outputs of elevation to local tidal record, amplitudes and phase lags for the 4 major constituents, M2, S2, K1 and O1 and the skill scores in Table 2a are shown. It shows the average relative errors of 5.1 % and 8.5 % for the amplitudes and phase lags, respectively. These skill scores demonstrate that the model performance is highly satisfactory. By using the estimated harmonic constants, non-harmonic constants are computed to obtain the tidal ranges at spring and neap tidal phases listed in Table 2b. Skill scores for the spring and neap tidal ranges at the Samchonpo tidal station are 96 % and 97 %, respectively.

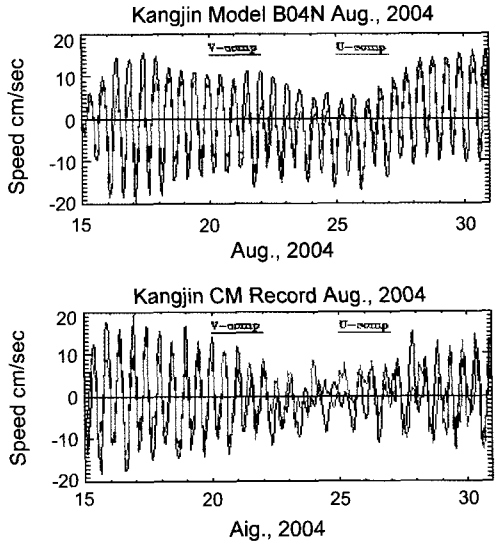

Fig. 3. Time series of observed and model predicted current in August, 2004 at Monitoring Station.

Time series of measured velocity components are shown with the model output at Mon. St. in Fig. 3. As seen in the neap-spring modulation of semi-diurnal sea level oscillation in Fig. 2, tidal velocity components also oscillate in a similar manner in Fig. 3 except for the fact that the observed current record shows more random-noisy fluctuations than the model predicted one. The

Table 3. Comparison between model output of tidal current and current meter records in terms of ellipse parameters.

Exp.	Tidal Const.	sema	semi	inc	pha
Observation	M2	12.8	-1.5	58.9	345.6
	S2	4.1	0.4	36.7	12.4
	K1	2.9	1.1	83.8	338.0
	O1	0.8	-0.4	42.5	210.2
Model	M2	14.6	-2.0	55.6	327.3
	S2	4.1	0.2	58.9	352.8
	K1	1.7	-0.3	72.5	38.5
	O1	1.4	0.02	47.1	144.6
Skill (%) 1-Rel. error	M2	86.5	67.9	99.1	94.9
	S2	99.5	60.7	93.8	94.5
	K1	58.8	30.3	96.9	83.2
	O1	22.8	2.5	98.7	81.8

Notions of sema, semi, inc and pha stand for the semi-major, semi-minor axes, angle of the inclination and phase relative to local meridional (135°E). (-) sign for semi indicates counter-clockwise rotation of tidal ellipse.

current meter records in the August, 2004 contained the density-driven current due to the fresh water release from the NG Dam. This fact is reflected in the skill scores of model predicted tidal current.

The skill analyses of the current are carried in terms of the semi-major and semi-minor axes of tidal ellipses, since they represent tidal current characteristics better than amplitude and phase parameters in Table 3. They show average skill scores of 67 % and 40 % for the sema and semi, respectively which are seemingly much lower than those of elevation. In fact, the skill scores for M2 and S2 show still high scores over 85 %. The poor skill scores are thus attributed to the K1 and O1 constituents, which have much smaller amplitudes when compared to the semi-diurnal constituents. The diurnal constituents are more likely to be under a bigger influence of the density current components driven by the water discharge, which will be simulated and analyzed in Part II (Ro *et al.* 2007b). Skill for the inc and pha show very high scores, indicating that the orientation of the major axis is realistically predicted with good phase relation. Overall assessment of the skill analyses are still regarded as satisfactory, considering the difficulties in model development which has to deal with very complicated geometry and three open boundary conditions. For detailed model validation, more comparison of the model outputs with current measurements in the various locations for other periods were carried out and can be referred to Jung (2007).

Simulation of Tide and Tidal Current

Time series of sea levels in Fig. 2 show the basic features of semi-diurnal tidal variation modulated by the neap-spring fortnight cycle. In the KB, the spring tidal range was 277.3 cm, occurring on 18th August, 2004, which is compared to 221.3 cm at the neighboring TY St., while those of neap tidal range were 90.5 cm in the KJ, and 74.6 cm at TY St., occurring on 24th respectively. Highest high water in the KB from model prediction for the month of August, 2004 is 297.8 cm with lowest low water at 27.6 cm, while those at TY St. were 248.5 and 27.2 cm. Tidal range at Mon. St. in the KJ is about 7 cm bigger than at Samchonpo grid point at spring and 7 cm smaller than at Samchonpo grid point at neap. Additionally, when tidal range in the KJ is compared to Tong-Young tidal station, it is about 56 and 15 cm bigger at spring and neap, respectively.

Tidal current distributions for the spring and neap cycles are shown in Fig. 3. The tidal currents in the KB are rather complicated due to their physical settings, such as complex coastline, bottom topography and three open boundaries. In most of the model domain, maximal tidal currents rarely exceed one knot regardless of tidal phase, except in the narrow channels. Strongest current exists in the northern part of the KB where current in the very narrow NR Channel dominates. Because of the three open channels, the current distribution varies remarkably depending on the location inside the bay.

Horizontal distribution of tidal current field at flood and ebb tidal phases for spring and neap is shown in Fig. 4. The current field in the KB can be delineated in five sub-areas such that 1) in NR Channel and Jinju Bay area, flow field is dominated by the strong tidal currents across the NR Channel which is deflected toward the KB to the southwest where tidal currents subside significantly due to its shallow bottom, 2) in the SB, flow is north/southward depending on the tidal phase which is connected to the DB Channel where currents become intensified due to narrowing channel with local islands, 3) the KB area is connected to the CS Channel whose width is less than 300 m at its narrowest point where strongest tidal currents exist exceeding 4.5 knots, 4) in the southeastern part of the model domain, namely Samchonpo area, the current field is relatively mild and weak, since it is connected to the open waters of the South Sea. Since this area is under strong influence of boundary conditions imposed, some

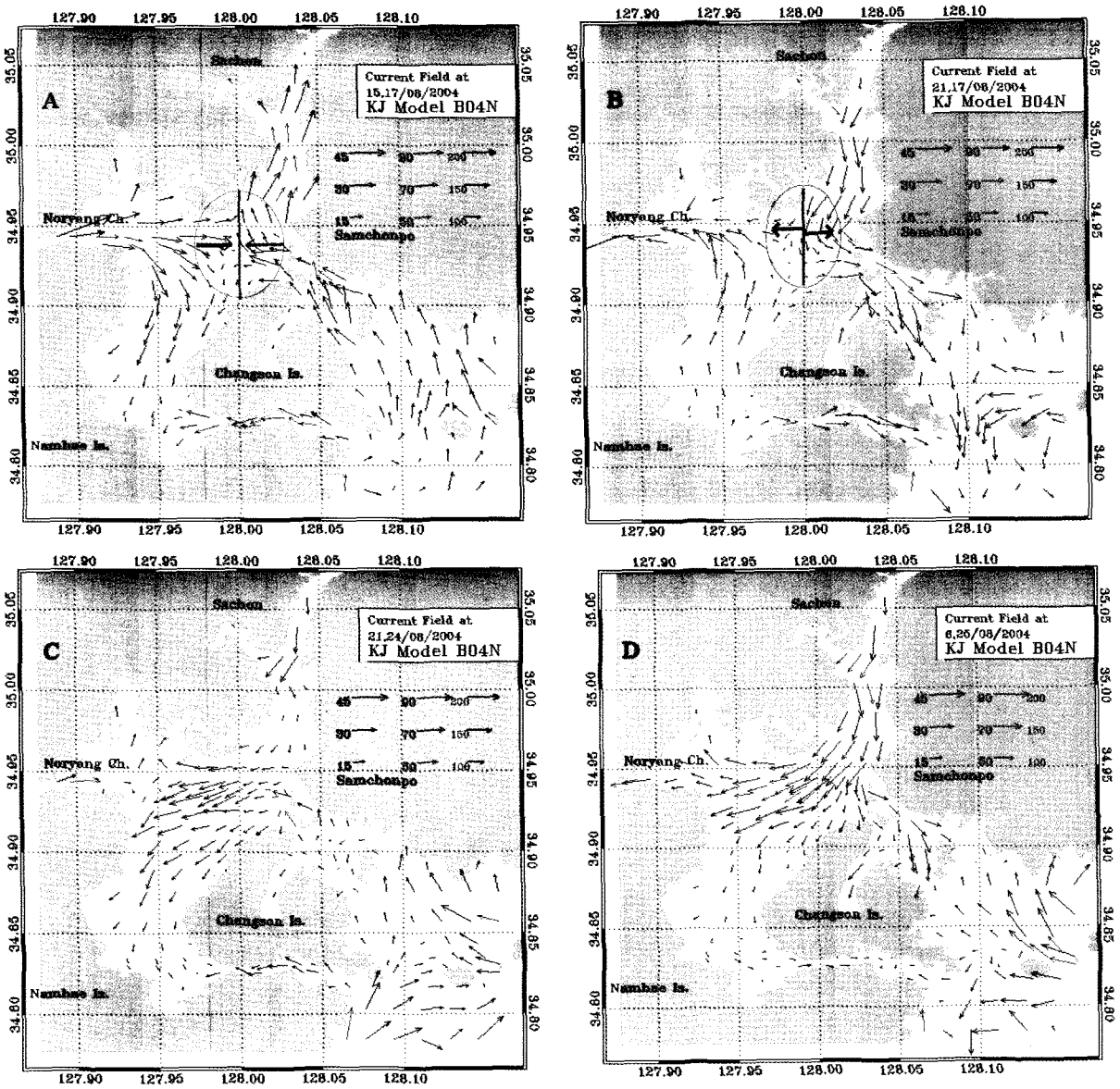

Fig. 4. Horizontal distribution of tidal current field. a: ebb, b: flood at spring, c: ebb d: flood at Neap, Aug., 2004.

fictitious current is reproduced at the corner points where unusual magnitude of velocity occurs; this should be neglected.

Another interesting feature associated with the tidal current field is the flow convergence (divergence) zone. There exists a line (marked in Fig. 4a) along which the water converges (diverges) at flood (ebb) phase of tide. The feature is a consequence of the local geometry and two channels of NR and DB. It is closely related to the residual recirculation cell to be discussed in the next section.

Fig. 5 represents the tidal ellipse characteristics in terms of semi-major, semi-minor axes, and inclination angle of the major axes relative to the north. Characteristics of the tidal ellipses in the KB can be summarized in that 1) most of the tidal currents are recti-linear with negligible semi-minor axis, 2) the orientation of the major axes are following the local isobaths, exhibiting the northeast-southwest axes mostly in the KB and SB areas, while in the Samchonpo area, they were northwest-southeast, and near Noryang and Changson Channels, they were east-west. 3) in the Chanson and DB Channel, biggest semi-major magnitudes exist, 4) in the mouth of the DB Channel, tidal ellipses show as more circular than anywhere else

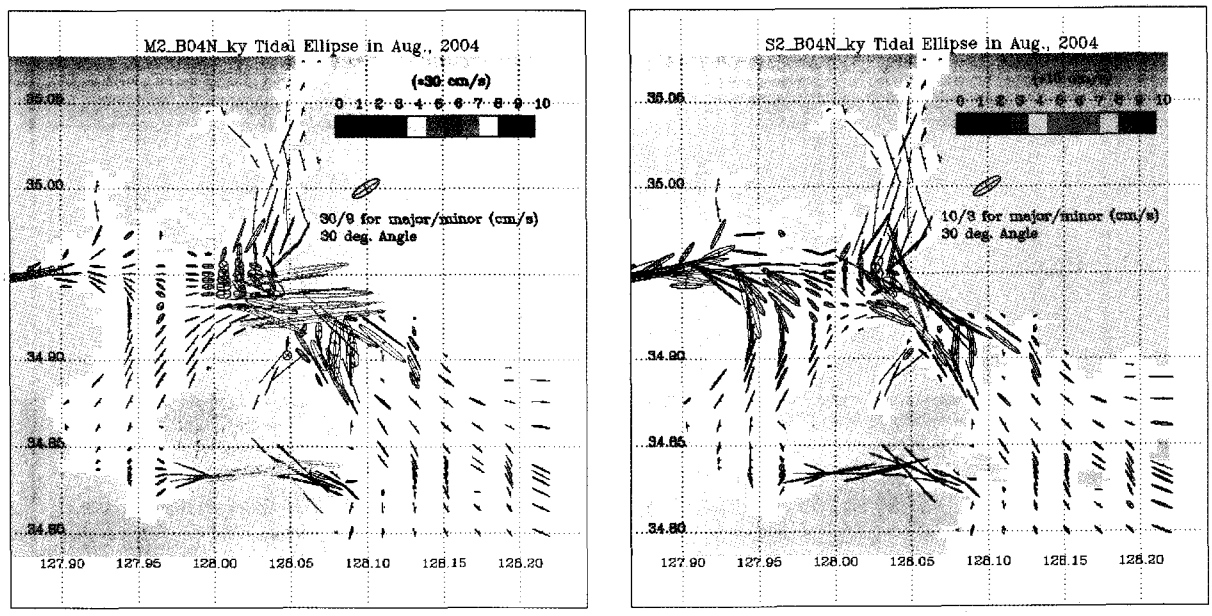

Fig. 5. Tidal ellipses for the M2 and S2 tidal constituents for the Run, B04N.

where the residual current forms the eddying motion. The ellipses of M2 and S2 resemble each other, however; the magnitudes of semi-major and minor for S2 are about half of the M2- note for the scale bar in the Fig. 5.

To represent the ellipse parameters in the KB, eight grid points are selected (Fig. 1) and Table 3 lists ellipse parameters in terms of semi-major, minor and inclination angle and phase lag for 4 major tidal constituents. Semi-major axes for M2 tidal current range from 1.7 to 38.5 cm/s, while semi-minor axes for M2 tidal current range from 0.1 to 7.5 cm/s. Semi-major axes for S2 tidal current range from 0.5 to 14.4 cm/s, while semi-minor axes for S2 tidal current range from 0.2 to1.2 cm/s. Ratio of S2 to M2 ranges from 0.2 to 0.6 while that of O1 to K1 ranges from 0.6 to 2.9. Eccentricity values for M2 range from 0.03 to 0.57, while that for S2 range from 0.09 to 0.53. As is obviously seen in Fig. 5, most of the tidal ellipses are rectilinear with eccentricity less than 0.2. A few locations are notable for their rotating tidal current at selected points of # 4 and # 6.

Tidal Residual Current Field

Fig. 6 represents the distribution of tidal residual current. Fig. 6a shows the mean tidal residual defined by the average of the residual current at each grid points. The pattern of the tidal residual current field can be summarized as follows; 1) in the SB, the dominant direction is southward with speed less than 5 cm/s, 2) in the JB, the residual entering from the NR Channel is to the east where it meets the water from the DB Channel which is directed to the west and the converging residual current flows southward into the KB, This feature, magnified in Fig. 6b, is most complex, yet interesting enough to deserve more thorough investigation. The sub-region, namely FA framed in Fig. 6b, lies at the mouth of the DB Channel just south of the SB and plays the role of a focal point where residual tidal currents converge from three directions; one from the west across the JB flowing eastward, and the other from SB flowing southward, and the last one from the DB Channel flowing northward. Due to the development of counter-clockwise eddy recirculation cell out of the DB Channel, neighboring residual currents are affected by this eddy and gradually drift to the west and then to the south.

Through the DB Channel, open ocean water is introduced into the model domain where bottle-neck effect is very strong and thus exhibits strong flood current reaching up to 5 knots in the spring tide (Fig. 4b). The converging water would flow southward along the northwestern coastline of the Changson Is. and would eventually flow out through the CS Channel into the open ocean.

Table 4 summarizes the statistics of the residual current of model run, B04N at 8 selected points. The average residual currents range from -2.9 to 3.4 for u-component

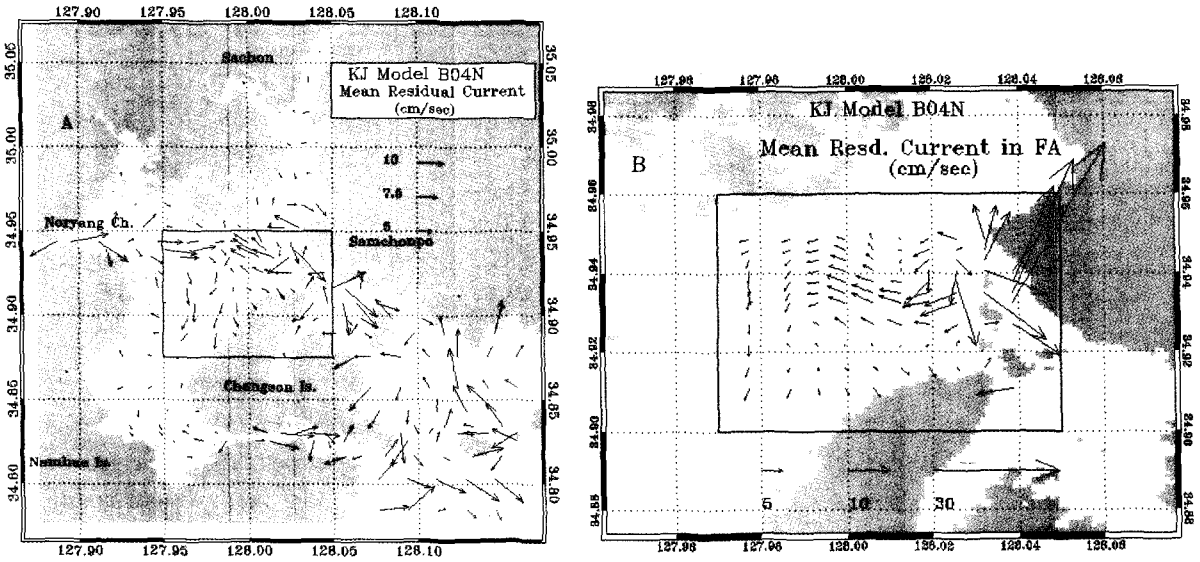

Fig. 6. Horizontal distribution of the tidal residual current field, A: Mean, B: magnified view of the residual current field for the FA sub-region. To avoid the plotting complexity, velocity arrows are re-sampled every 4 grid points in Fig. 6a, while in Fig. 6b, same but every 2 points.

Table 4. Tidal ellipse parameters for 4 major tidal constituents at selected grid points.

Pt.	M2				S2			
	Sema (cm/s)	Semi (cm/s)	inc (deg)	pha (deg)	Sema (cm/s)	Semi (cm/s)	inc (deg)	pha (deg)
1	38.5	-3.1	57.2	70.1	14.4	-1.2	52.7	113.5
2	11.7	2.5	0.3	90.5	3.1	1.3	15.7	203.8
3	13.2	-7.5	115.7	38.4	2.6	-0.4	95.2	153.0
4	6.9	1.6	54.9	223.9	3.2	-1.0	58.2	271.2
5	23.5	-3.1	109.4	52.7	8.0	-0.8	111.7	89.9
6	1.7	-0.1	5.7	0.0	0.5	-0.3	151.6	332.0
7	22.2	0.5	22.7	224.6	9.3	0.2	22.6	273.2
8	7.8	-2.2	78.7	48.6	4.7	-0.6	33.2	248.6
	O1				K1			
1	3.0	-0.03	50.6	46.5	3.1	-0.37	57.4	20.4
2	2.6	0.04	5.8	104.4	0.9	0.09	157.0	207.0
3	1.0	-0.11	59.7	54.2	1.1	-0.22	122.5	288.5
4	0.7	0.05	31.5	157.8	0.6	0.17	67.6	180.3
5	1.2	-0.03	125.5	29.9	1.8	0.04	117.1	12.3
6	0.3	0.02	143.9	275.0	0.4	-0.03	141.2	316.9
7	2.0	0.00	18.0	208.0	2.4	-0.06	20.4	201.9
8	4.1	0.65	51.2	262.7	2.6	-1.07	53.9	113.8

and -4.5 to 3.8 for v-component, respectively. In spite of the small magnitudes of the residual current, the standard deviations show rather large values ranging from 0.8 to 7.0 for u-comp. and 0.6 to 10.7 for v-comp. At the pt # 8 which is located inside of the CS Channel, the maximal residual current exceeds 35.0 cm/s, which is considered to be a big value. As is expected in the results of mean residual current field, the asymmetry between ebb and flood phases is obvious so that depending on the locations, tidal currents can be classified either as ebb-dominant(E) or flood-dominant(F), listed in Table 5.

4. Discussion and Summary

Sea level oscillation simulated by the model could account for the 95 % of the tidal records measured at the

Table 5. Basic statistics of residual current of model run, B04N at the selected points.

Pt. #	U-comp. (cm/s)				V-comp. (cm/s)				Type
	Mean	st. dev	Mini	Maxi	Mean	st.dev	Mini	Maxi	
1	0.4	4.5	-24	13.4	1.4	5.3	-32.8	15.3	F
2	1.6	5.6	-19.5	17.9	0.2	2.8	-7.2	9.6	F
3	1.4	7.0	-22.1	26.8	-4.5	4.4	-15.3	7.5	E
4	0.1	2.1	-5.5	7.9	-0.7	2.4	-5.8	8.0	E
5	-2.9	2.4	-10.5	7.9	-3.4	5.5	-20.4	19.9	E
6	0.5	0.8	-2.0	4.1	0.0	0.6	-2.3	1.9	E
7	-2.9	3.8	-15.5	25.4	1.1	1.5	-5.2	10.0	F
8	3.4	5.9	-11.2	20.3	3.8	10.7	-24.4	35.0	F

Samchonpo tidal station located in the middle-eastern part of the model domain. The tidal current field reproduced by the model demonstrates the complexity of the flow system in the KB. However, the flow regimes could be well described in term of five sub-regions so that in the northern part of the domain, at the ebb phase, the water from the SB is diverged into two paths, one directing to the NR Channel westward and the other flowing southward into the DB Channel, whereas in the southern part, the water in the KB flows out into southern open ocean water through the narrow CS Channel. At flood phase, the flow is reversed almost 180 degrees, which is seen in Fig. 5, showing the tidal current strongly recti-linear with the major-axis parallel with the local iso-bath.

Tidal current characteristics can be understood in the tidal ellipse parameters depicted in Fig. 5 for M2 and S2 constituents. The semi-major axes of the ellipse for M2 range from 1.7 to 38.5 cm/s and S2 range from 0.5 to 14.4 cm/s. In general, the semi-major axes of S2 are around 50 % of those of M2 in the KB. The eccentricity of ellipse for M2 and S2 are 0.2 and 0.23 on the average, respectively illustrating that the tidal current in the KB is strongly recti-linear. However, there are some locations where more elliptical circles exist at the mouth of the DB Channel, thus flow patterns are more rotational and exhibit eddy-like motions. This feature is closely related to the residual current pattern in this sub-region discussed in the following paragraph.

The tidal residual current in the model domain is complex and varies greatly depending on the location. However, in the sub-region, at the mouth of the DB Channel just south of the SB, lies a focal point where residual currents converge from three directions: one from the west across the JB flowing eastward, and the other from SB flowing southward, and the last one flowing northward from the DB Channel out of which a counter-clockwise eddy recirculation cell is developed. The converged water should flow southward along the northwestern coastline of the Changson Is. and would eventually flow out through the CS Channel into the open ocean.

This study is based on the numerical modeling experiments for the sea level oscillation in the tidal current field in the KB. The model outputs were compared to the measured sea level and tidal current records. The skill scores of the sea level show the performance grades over 90 % for each of four major tidal constituents (M2, S2, K1, O1) in terms of amplitudes and phases. In contrast, skill scores for the tidal ellipse parameters in terms of sema and semi range from 22.8 to 99.5 % and 2.5 to 67.9 %, respectively. However, most energetic constituents such as M2 and S2 were reproduced with skill scores over 86 % for sema. Therefore, the performance of the developed numerical model in the KJ is assessed as fairly successful. This is considered a big step forward toward understanding the dynamics in the KB, which would form a basis to further develop the simulation of current driven by the fresh NG Dam water discharge and its impact on the formation of the hypoxia in the bottom waters which would be dealt with in a following paper (Ro *et al.* 2007).

Acknowledgement

This study (MNF 22003011-3-2-SB010) was funded by the MOMAF administered by Korea Institute of Marine Science & Technology Promotion. The first author expresses his gratitude to the two reviewers (one anonymous and Dr. Tae In Kim) for their valuable comments and indications which helped to clarify the description parts of the model calibration and validation.

References

Blumberg, A. F. and G. L. Mellor. 1987. A description of a three-dimensional coastal ocean circulation model. p. 1-16. In: *Three-Dimensional Coastal Ocean Models, Coastal Estuarine Sci.*, vol. 4, ed. by N. S. Heaps, AGU, Washington, D. C.

Blumberg, A.F., L.A. Khan, and J.P. John. 1999. Three-Dimensional Hydrodynamic Model of New York Harbor Region. *J. Hydr. Eng.*, **125**(8), 799-816.

Cai S., Q. Huang, and X. Long. 2003. Three-dimensional numerical model study of the residual current in the South China Sea. *Oceanologica Acta,* **26**(5), 597-607.

Fong, D. A. 1998. Dynamics of freshwater plumes: Observations and numerical modeling of the wind forced response and along-shore freshwater transport. Ph.D. thesis, MIT/WHOI Joint Program in Oceanography, Woods Hole.

Foreman, M.G.G. 1978. Manual for Tidal Current Analysis and Prediction. Pacific Marine Science Report 78-6, Institute of Ocean Sciences, Patricia Bay, Victoria, B.C. 39 p.

Gomez-Valdes, J., J.A. Delgado, and J.A. Dworak. 2003. Overtides, compound tides and tidal-residual current in Ensenada de la Paz Lagoon, Baja California Sur, Mexico. *Geophysica Int.,* **42**, 623-634.

Horrevoetsa, A.C., H.H.G. Savenijea, J.N. Schuurmana, and S. Graasa. 2004. The influence of river discharge on tidal damping in alluvial estuaries. *J. Hydrol.,* **294**, 213–228.

Ji, Z. G., G. Hu, J. Shen, and Y. Wan. 2007. Three-dimensional modeling of hydrodynamic processes in the St. Lucie Estuary. *Estuar. Coast. Shelf Sci.,* **73**, 188-200.

Jung, K.Y. 2007. Three-Dimensional Numerical Modeling of Tidal, Wind-Driven and Density Currents in the Kangjin bay, South Sea, Korea. M.S. thesis, Chungnam National University. 130 p.

Kourafalou, V.H., L. Oey, J. Wang, and T.N. Lee. 1996a. The fate of river discharge on the continental shelf, 1, Modeling the river plume and inner shelf coastal current. *J. Geophys. Res.,* **101**, 3415-3434.

Kourafalou, V.H., T.N. Lee, L. Oey, and J. Wang. 1996b. The fate of river discharge on the continental shelf, 2, Transport of coastal low-salinity waters under realistic wind and tidal forcing. *J. Geophys. Res.,* **101**, 3435-3456.

Levasseur, A., L. Shi, N.C. Wells, D.A. Purdie, and B.A. Kelly-Gerreyn. 2007. A three-dimensional hydrodynamic model of estuarine circulation with an application to Southampton Water, UK. *Estuar. Coast. Shelf Sci.,* **73**, 753-767.

Matsumoto, K., T. Takanezawa, and M. Ooe. 2000. Ocean Tide Models Developed by Assimilating TOPEX/POSEIDON Altimeter Data into Hydrodynamical Model: A Global Model and a Regional Model Around Japan. *J. Oceanogr.*, **56**, 567-581.

McLaughlin, J.W., A. Bilgili, and D.R. Lynch. 2003. Numerical modeling of tides in the Great Bay Estuarine System: Dynamical balance and spring–neap residual modulation. *Estuar. Coast. Shelf Sci.,* **57**, 283-296.

Marinone, S.G. and M.F. Lavýn. 2005. Tidal current ellipses in a three-dimensional baroclinic numerical model of the Gulf of California. *Estuar. Coast.Shelf Sci.,* **64**, 519-530.

Mellor, G.L. and T. Yamada. 1982. Development of a turbulence closure model for geophysical fluid problem. *Rev. Geophys. Space Physics,* **20**, 851-875.

Odamaki, M. 1989. Tides and Tidal Current in the Tusima Strait. *J. Oceanogr. Soc. Japan,* **45**, 65-82.

Orlanski, I. 1976. A simple boundary condition for unbounded hyperbolic flows. *J. Comput. Phys.,* **21**, 251-269.

Park, K., H.S. Jung, H.S. Kim, and S.M. Ahn. 2005. Three-dimensional hydrodynamic-eutrophication model (HEM-3D): Application to Kwang-Yang Bay, Korea. *Mar. Environ. Res.,* **60**(2), 171-193.

Pawlowicz, R., B. Beardsley, and S. Lentz. 2002. Classical tidal harmonic analysis including error estimates in MATLAB using T_TIDE. *Comput. Geosci.,* **28**, 929-937.

Ro, Y.J. 2006. Internet-based Realtime Monitoring of the Environmental Parameters in the Marine Large-Arc Shell Culture Bed and Its Productivity Assessment Model, Final Report, Ministry of Maritime Affairs and Fisheries. 155 p.

Ro, Y.J. 2007. Tidal and Sub-tidal Current Characteristics in the Kangjin Bay, South Sea, Korea. *Ocean Sci. J.,* **42**(1), 19-30.

Ro, Y. J., K.H. Na, and C. K. Kim. 2004. 1st year Interim report for the Internet based Realtime Monitoring of the Oceanic Condition in the Kangjin Bay for Aqua-culture and its Productivity Estimation submitted to KMI, MOMAF. 95 p.

Ro, Y.J. and K.Y. Jung. 2007. 3-D Baroclinic Numerical Modeling of River Plume and Density Current due to Dam Water Discharge. To be submitted to *Ocean Science Journal.*

Ro, Y.J. and Y.H. Choi. 2004. Application of the Realtime Monitoring of Oceanic Conditions in the Coastal water for Environmental Management. *J. Korean Soc. Oceanogr.,* **39**(2), 148-154.

Ro, Y.J., W.S. Jun, K.Y. Jung, and B.H. Kim. 2005. Numerical Modeling of River Plume in the Kangjin Bay and Its Implication for the Ecosystem. Proc. of Autumn Meeting, 2005 of the Korean Society of Oceanography, Nov. 3-4, 2005, Ansan, Korea, 218-220.

Smagorinsky, J. 1963. General circulation experiments with the primitive equations, I. The basic experiments. *Mon. Weather Rev.,* **91**, 99-164.

Valle-Levinson, A. and T. Matsuno. 2003. Tidal and subtidal Flow along a Cross-shelf Transect on the East China Sea. *J. Oceanogr.*, **59**, 573-584.